DEVELOPMENT OF A TOOL TO MEASURE BOND-LINE READ-THROUGH

Kedzie Fernholz[1], Réda Hsakou[4], Kim Lazarz[1], C.S. Wang[2], Bob Emerson[3], Dave Biernat[3], Darryl Case[5]

[1]Ford Motor Company, Dearborn, MI USA (kfernhol@ford.com)
[2]General Motors Corporation, Warren, MI USA
[3]DaimlerChrysler Corporation, Auburn Hills, MI USA
[4]Visuol Technologies, Metz, France
[5]EOS Technologies, Auburn Hills, MI USA

Abstract

The Automotive Composites Consortium Joining Working Group (ACCJWG) teamed with Visuol Technologies and EOS Technologies to develop a measurement system for quantifying the severity of "bond-line read-through" (BLRT). BLRT is a visual defect that can occur when two panels are bonded together. The measurement system is based on the ONDULO technology developed by Visuol Technologies. To develop the metric, the ACCJWG provided Visuol Technologies a set of forty-eight panels with varying amounts of BLRT. Curvature maps for each of the panels were captured using the ONDULO technology. Visuol Technologies then used the information in the curvature maps to develop an algorithm for calculating a BLRT "score" that quantifies the severity of the defect.

The algorithm first filters out any pixels in the curvature map below a certain magnitude. The remaining pixels are grouped by their proximity to one another to create discrete defects. Since there were many small defects found in the curvature maps, a defect's mean amplitude and aspect ratio are required to fall within certain thresholds to be included in the final score. The score for each individual defect is the product of its mean amplitude, size, and aspect ratio. The final BLRT score for a panel is a sum of the scores for each defect on the surface.

Since the original algorithm was developed using panels made with continuous beads of adhesive, the algorithm is being modified to properly assess other types of defects. For the set of panels used to develop the initial algorithm, the score developed was shown to correlate well to the visual assessment of the panels. Furthermore, since the metric is based on measured physical characteristics of the defects, it provides a unique method for objectively quantifying the severity of BLRT defects.

Introduction

The appearance of an automobile's exterior is one of the most important factors to a customer when they are choosing which vehicle to purchase. Consequently, manufacturers work hard to ensure that the surface produced is the Class "A" surface intended. While there are many benefits to using adhesives in automotive body components, their use can cause a distortion in a Class "A" surface. This distortion appears as a visible surface defect that has been termed "bond-line read-through" (BLRT).

There have been many efforts to determine what causes this distortion in a surface [1-4]. Unfortunately, the results of many experiments appear to contradict each other. This is most likely due to the fact that an instrument capable of objectively quantifying the severity of BLRT

did not exist. Consequently, to conclusively determine the causes of BLRT and to develop a tool to model it, an instrument capable of objectively quantifying the severity of BLRT in a way that correlates to visual assessment needed to be developed.

The Automotive Composites Consortium Joining Working Group (ACCJWG) began a project to develop a fundamental understanding of BLRT in 2005. The group initially evaluated several different technologies for their potential ability to objectively quantify BLRT. Initial evaluation of the ONDULO technology demonstrated that the output is much more sensitive than the human eye. Unfortunately, none of the metrics that already existed in that software produced a value that correlated to our visual assessment of the panels. Consequently, the ACCJWG collaborated with Visuol Technologies and EOS Technologies to develop a new metric capable of providing an objective measure of this defect.

The ONDULO Technology

The ONDULO technology is based on the principle of deflectometry. The basic principle of deflectometry is visible everyday. Consider the image in Figure 1. The windows of this building do not reflect the real design of the church. Our eyes perceive the distortion in the reflection as abnormal. This illustrates the concept that by evaluating the distortion of a reflection on a surface, one can obtain information about the distortion in the surface itself.

Figure 1. A Reflection on Building Windows.

The automotive industry applies the same principle to analyze the appearance of exterior body panels. A Class “A” quality surface is defined as a high-quality surface with no undesirable waviness. Human inspectors look for distortion of a regular light pattern to determine whether there are any unacceptable defects in the panels, as shown in Figure 2. Unfortunately the inherent variability between human inspectors means that this subjective method of evaluating panels is not capable of ensuring a consistent, objective measurement of the quality of a surface.

Figure 2. Visual inspection of paint quality in an automotive plant.

In a Class "A" surface, the curvature of the surface is designed to be continuous in each direction, except at character lines. That means that on the majority of the surface each point along a common line should have the same radius of curvature.

Locally, any surface can be defined by the function z = f(x,y). The slope of the surface can be defined by its components $\partial z/\partial x$ and $\partial z/\partial y$. The slope variation from one point to the other is described by the two components $\partial^2 z/\partial x^2$ and $\partial^2 z/\partial y^2$ (the slope derivatives) as well as by the cross-derivative $\partial^2 z/\partial x \partial y$ (the torsion). This is illustrated in Figure 3. The torsion cross-derivative term will not be taken into account in the ONDULO calculations.

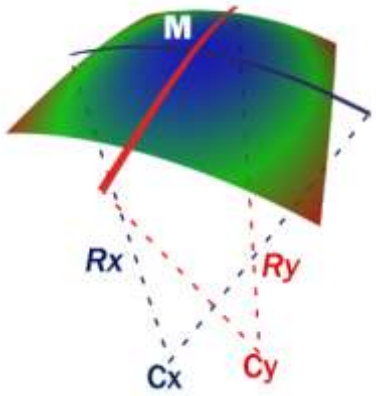

The slope derivatives $\partial^2 z/\partial x^2$ and $\partial^2 z/\partial y^2$ are the curvatures k_x and k_y, which are the reciprocal of the radius of curvatures R_x and R_y.

$$k_x = \frac{\partial^2 z}{\partial x^2} = \frac{1}{R_x}$$

and

$$k_y = \frac{\partial^2 z}{\partial y^2} = \frac{1}{R_y}$$

Figure 3. Curvature of a Surface at a Point.

The importance of the curvature to the apparent severity of a defect is illustrated in Figures 4 and 5. Figure 4 shows the actual shape of a surface compared to its nominal shape. First consider the large, gradual deviation across the whole part. While the actual shape deviates from the nominal shape, an observer is unlikely to identify this large, gradual variation from the nominal. On the other hand, a very sharp deviation, or "bump", introduces a local, high frequency distortion that will be identified as an aesthetic defect. Examples of this type of defect are "dirt in paint", pinholes, and BLRT. Figure 5 illustrates the importance of the ratio between the altitude and the wavelength to the apparent severity of a defect. This figure shows two defects with identical altitude (cross-section z). The second defect, however, appears to be

more severe because its curvature (cross-section d^2z/dx^2) is larger. Both of these figures illustrate the importance of characterizing an appearance defect by the spatial derivative of its slope, i.e. its curvature, rather than by its altitude. Thus, the advantage of using deflectometry is that it allows the local curvature variation to be quantified and it is the local curvature variation that is the most relevant criterion for surface appearance analysis. Deflectometry also allows one to make use of a high ratio between the field of view and sensor size. This results in a high spatial resolution and thus better correlation with visual perception.

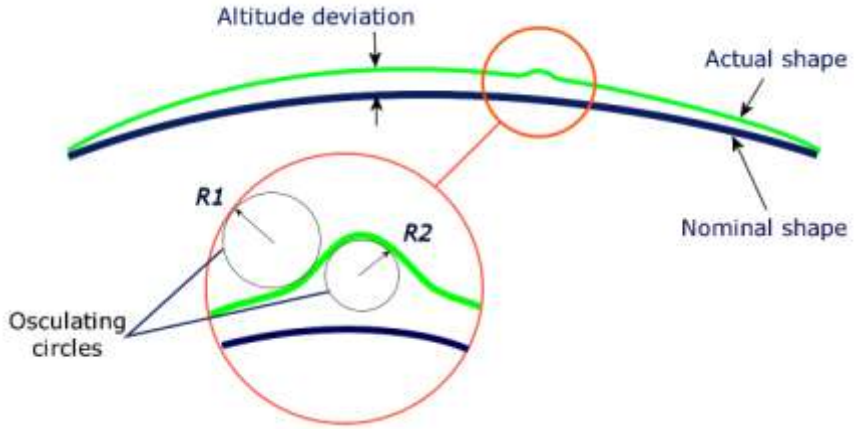

Figure 4. Altitude deviation and curvature.

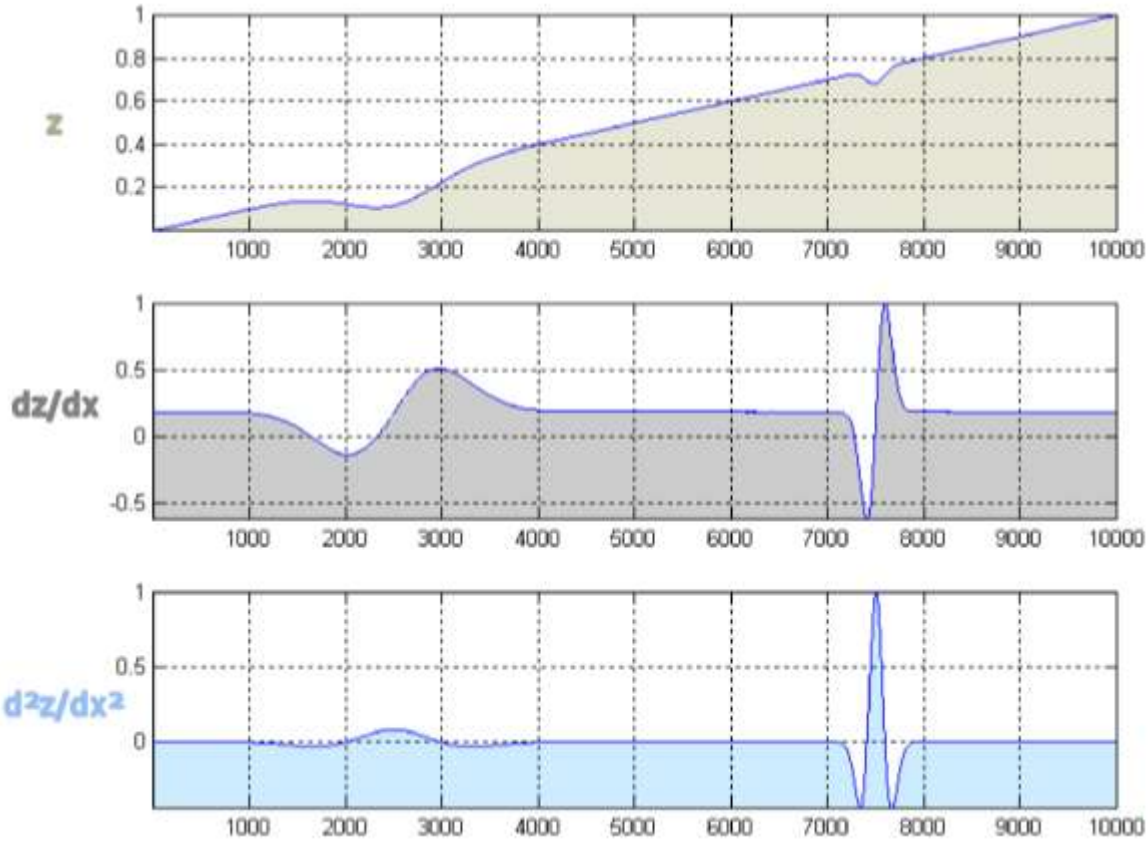

Figure 5. Visual relationship between altitude, slope and curvature.

The ONDULO technology is designed to replace subjective visual evaluations with a non-contact optical technique. By replacing the eye with a high resolution camera, the goal of the measurement technique is to quantify the local distortion of the reflection for each pixel of an image of a surface by calculating the local curvatures. The curvature information from a surface can then be quantified in a way that is objective and correlates to subjective evaluations.

To obtain a measurement, a regular fringe pattern is displayed on a screen (not projected on the sample as is done in a classical fringe projection system). The regular fringe pattern, or grid, displayed on the screen can be thought of as a luminous graduated ruler. The fringe pattern displayed is a sinusoidal signal with the known period *p.* The camera is focused on the part to be evaluated and captures the reflected image of the grid. This is illustrated in Figure 6.

Figure 6. Distortion of a Reflected Grid as Seen on a Bumper.

For each point M(x,y) of the reflection on the surface, the sinusoidal behaviour of light intensity is represented by the following equation:

$$I(x,y) = Io(x,y).[1 + \varphi(x,y).\cos(\Phi(x,y) + \Delta\Phi(x,y))]$$

Io: average ambient local intensity
φ: contrast of the fringes
Φ: phase of the considered point

Since the light pattern displayed on the screen and reflected from the measured surface has a sinusoidal signal with a known period *p*, it is possible to extract the phase variation, ΔΦ, by phase shifting. The phase variation is the first geometrical variable to be determined for each point of the distorted reflection.

Since the light intensity equation above has four unknown values (Io, φ, Φ, and ΔΦ), it is necessary to identify at least four equations to solve the problem for each point M(x,y). The "temporal" approach used in the ONDULO technology consists of evaluating the unknown parameters for the same point M(x,y) on the surface each time the grid is displaced by phase shifting. The grid is shifted and a new image is captured. This allows one to measure several intensities I_k, k = 0, 1,…, n-1 at each point. A minimum of four intensities is needed to solve the

system of equations. Since the grid is shifted by a controlled amount, each measurement is separated by a constant phase variation δ: $I_k = I(\Phi + k\delta)$, which corresponds to the phase variation ΔΦ.

Each light intensity, I(x,y), coming from a reflected ray of light is measured by one pixel of the CCD chip in the camera which then converts this light intensity into electronic signals to send to the ONDULO software. Depending on the camera resolution, the output of the camera (in this case the light intensity value integrated by each pixel of the CCD) is digitized into an array of pixels, each having a specific grey level (GL) value. The grey level ranges from 0 to 255 GL. Consequently, the light intensity input being sent to the software is scaled by GL.

With the matrix of 'k' equations and 'k' known values, I_k, obtained by the multiple measurements obtained by phase shifting, the values for Io, φ, Φ and ΔΦ can be calculated for each point M(x,y) of the surface.

The value for ΔΦ at each point M(x,y) is obtained by solving the system of equations. ΔΦ corresponds, more or less, to the local slope at that point. To accurately quantify the ΔΦ value, known geometrical parameters of the setup configuration (distances, angles, etc) will be needed. The setup configuration gives the location of the light source point on the grid and, with the phase shifting, provides the spatial displacement, *Δu,* between the light source if no defect is present, and the light source if a defect is present. The presence of a defect will cause a change in orientation of the normal to the point M(x,y), α, as illustrated in Figure 7. This change in orientation of the normal is equal to the local slope, dz/dx.

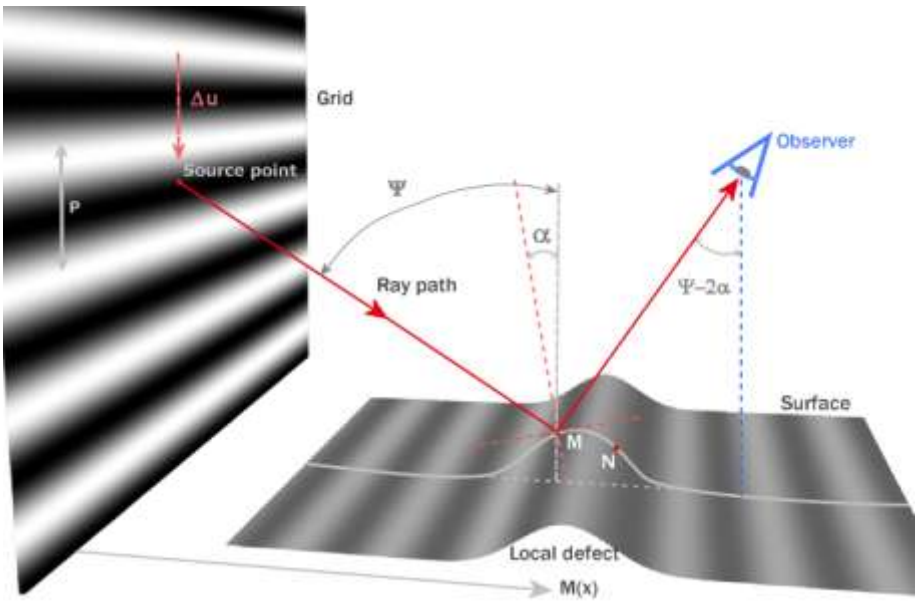

Figure 7. Effect of the Local Slope on the Reflection.

As the position of the point on the grid varies with a rate of 2π per *p*, the phase variation ΔΦ corresponding to *Δu* is such that: ΔΦ = 2π.Δu/p. The slope α. is given by the relation: $2\alpha = 2\tilde{.}d(\Delta z)/dx = \Delta u/M(x)$.

To quantify the curvature value of the point M(x,y), the equation $\alpha = s(x).\Delta\Phi(x)$ defines the relationship between the phase shifting ΔΦ and the slope α where the coefficient s(x) = p4∏M(x) is the measurement sensitivity. Then the value of the curvature for the point M(x,y) is calculated by derivation of the slope.

BLRT Samples

The ACCJWG manufactured seventy-two panels by bonding 2.5 mm thick SMC hat sections to flat 2.0 mm thick Class "A" SMC plaques. A schematic of the panel geometry is shown in Figure 8. Assemblies were fabricated so that the panels would exhibit varying amounts of BLRT.

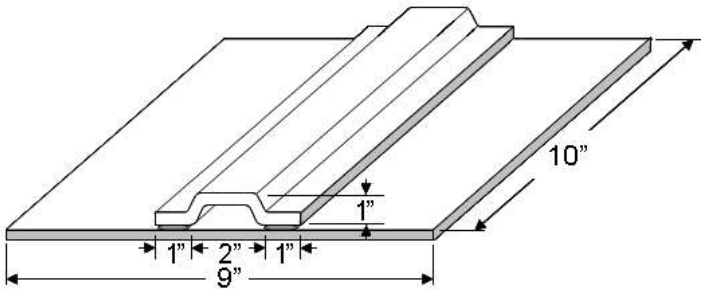

Figure 8. BLRT Panel Schematic.

Half of the hat sections used were molded using low density structural SMC. The other half were molded using regular density structural SMC. Panels were bonded using one of two different adhesives. The bond gap was fixed at 0.8 mm using Teflon coated metal shims at each end. The shims were removed after the adhesive was cured. Adhesive was applied to the panels by hand. The intent was to apply sufficient adhesive to create squeeze-out. In half of the panels, the squeeze-out was removed. Assemblies were cured at either room temperature or for 10 minutes at 285°F. Three panels were fabricated using each combination of conditions. One of each replicate was left in the "as-bonded" ("raw") state and the other two were primed. After priming, one of the two primed panels of each type was painted black.

After priming and painting, twelve panels from each condition ("raw", primed, and painted) were chosen. The panels included in the primed and painted sets were selected so that the set contained panels with a range of BLRT severities. BLRT was difficult to see with the unaided eye in the raw panels, so the raw panels chosen were those made at the same conditions as those in primed panel set.

In addition, twelve panels from an earlier BLRT study at Ford were included in this evaluation. There were approximately 200 panels in that set. All had been painted white. In that study, the panels had been evaluated with the Diffracto system, another surface quality evaluation method. Panels borrowed from that work for this study had BLRT that was not readily visible with the unaided eye. Panels with D-sight scores between 100 and 1200, spaced approximately 100 units apart, were chosen. A 100 unit difference is thought to be relatively small, but this resulted in a distribution of panels that was assumed to cover the range of BLRT below the visible limit.

Visual Evaluation of the BLRT Samples

BLRT was not visible to observers on the “raw” and painted white panels. This was not because BLRT was not present on the panels but rather because of the surface characteristics of the panels made it difficult for the human eye to perceive the flaws. BLRT defects are difficult to see on raw panels because of the low level of reflection from the surface. These defects are difficult to see on white painted panels because of the relatively low contrast between the defect and the surrounding area. The defect is visible on the primed panels because of the higher level of contrast and on the painted black panels because of both a higher level of contrast and a high level of reflection.

Since BLRT was visible on the twelve primed and twelve painted black panels, a thirty person jury ranked each set of panels to provide visual assessment data. The jury was asked to rank the BLRT from the least severe to the most severe (1 to 12) in each set. This data was then used as the benchmark to which the developed metric was expected to correlate.

The jury evaluation demonstrated the difficulty in visually assessing the severity of this defect. Even though jurists were asked only to rank the severity of the defect on the panels relative to each other, there was still a considerable amount of scatter in the data. Figures 9 and 10 illustrate the results from the jury evaluation. Groups of panels that had a severity that was statistically indistinguishable are shown with a line below them. Note that many of the groups overlap. This means that, for instance, the severity of BLRT on primed panel 44 was statistically equivalent to that on both panel 5 and 32, but yet the defect on panel 32 was “more severe” than the defect on panel 5. The amount of variation in the jury results indicates that while the rating developed for BLRT should correlate to the jury’s assessment, there is room for some deviation between the rankings shown in Figures 9 and 10 and the rankings that result from the developed BLRT “score”.

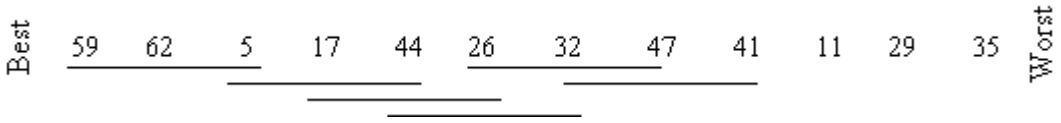

Figure 9: Illustration of the Rankings from the Jury Evaluation of the Primed Panels

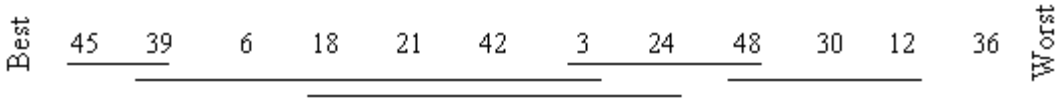

Figure 10: Illustration of the Rankings from the Jury Evaluation of the Painted Panels

ONDULO Evaluation

The forty-eight panels were imaged using the ONDULO technology. The data was first filtered using several existing ONDULO algorithms. Visual evaluation of the resultant curvature maps showed that surface features with a wavelength less than 5 mm were not related to BLRT. Consequently, the curvature maps were filtered to remove these wavelengths from the data. Curvature maps containing structures with wavelengths greater than 5 mm, wavelengths between 5 mm-20 mm, and wavelengths between 20 mm-40 mm were examined and considered when developing the BLRT metric.

One promising result from the imaging was confirmation that the ONDULO technology is insensitive to surface finish. The surface finish of a panel will greatly influence a person's ability to see a defect because of the impact the surface finish has on the contrast between a defect and the surface. Nevertheless, it is important to have a measurement tool that is capable of measuring defects that are below the visible limit. This is particularly true with defects that are difficult to see because of the surface finish of the panel rather than because of the defect's severity.

When the team initially looked at the "raw" panels and the "painted white" panels, those panels were determined not to have visible BLRT. When the panels were imaged with the ONDULO technology, though, the severity of the BLRT on some of the panels in both of these sets appeared to be similar to that seen on some of the panels in the primed and painted black sets. In fact, the BLRT on the "raw" panels appeared to be quite similar to that on the other panels made at the same conditions. Figures 11-13 are curvature maps of raw, primed, and painted panels made using the same materials and processing conditions as an example.

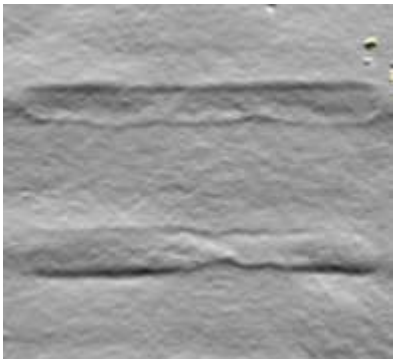

Figure 11: Curvature Map for Raw Panel 34

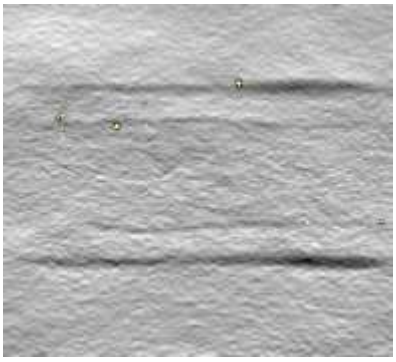

Figure 12: Curvature Map for Primed Panel 35

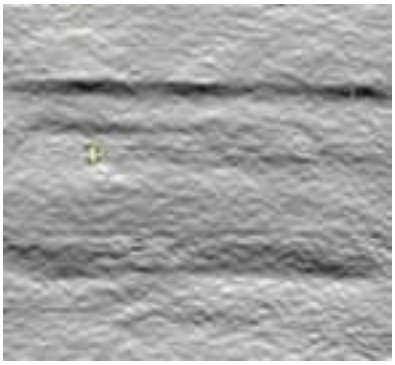

Figure 13: Curvature Map for Painted Panel 36

Visual Evaluation of the Curvature Maps

The curvature maps produced by the ONDULO technology demonstrated one of the likely reasons that there was so much variation in the jury rankings of the primed and painted black panels. Figures 14 and 15 are curvature maps from two black painted panels. These curvature maps contain only defects with a wavelength greater than 5 mm. There are small yellow areas at the bottom of these images that are due to dirt in paint and should be ignored.

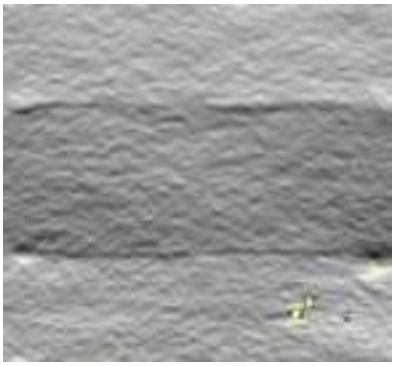

Figure 14: Panel 3 Curvature Map

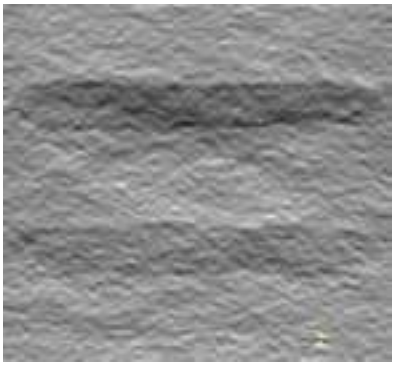

Figure 15: Panel 42 Curvature Map

These two figures illustrate some of the differences seen in the BLRT "signature" on the various panels included in this work. It is difficult to determine subjectively whether the "distinct" defect in Figure 14 is "more visible" than the "diffuse" defect in Figure 15. Accordingly, in the jury responses for the visual evaluation of the actual panels, these two particular panels were ranked in every position (1-12) by at least one person in the jury. Not surprisingly, when the ranks were averaged, these two panels were ranked #7 and #6 overall. Because of the variation in the rankings, though, these average scores may have simply been the result of regression to the mean. Consequently, in these cases the jury data doesn't necessarily provide much assistance in determining which type of defect is more visible.

Since there was so much variation in the jury's assessment of the relative ranking of the panels, the ACC team members attempted to rank the severity of the defects as seen on in the curvature maps. That ranking was completed on all three types of curvature maps (wavelengths greater than 5mm, wavelengths between 5 mm-20 mm, and wavelengths between 20 mm-40 mm).

Two problems were encountered when trying to establish the "proper" ranked order based on the curvature maps. First, people are not necessarily able to correctly determining whether a defect that appears white (an "indent") is "more" or "less" severe than one that appears black (an "outdent"). Figures 16 and 17 illustrate two curvature maps with defects of "similar" severity but different coloring.

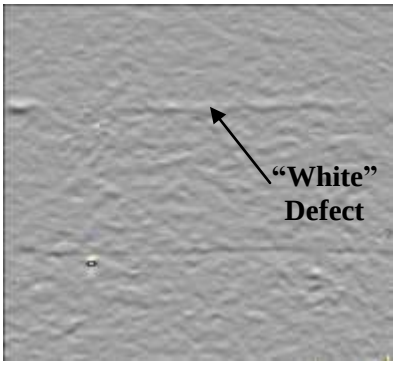

Figure 16: Panel 4 Curvature Map

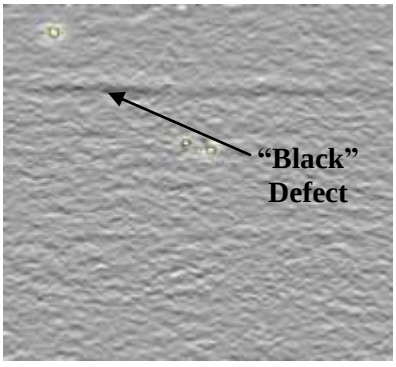

Figure 17: Panel 41 Curvature Map

Second, the "background" color can differ between curvature maps, as shown in Figures 18 and 19. It is very difficult for people to look at these two maps and know which defect should be considered as being "worse".

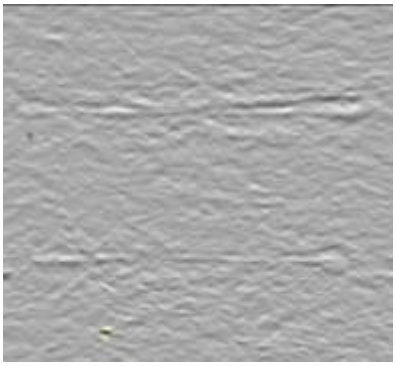

Figure 18: Panel 31 Curvature Map

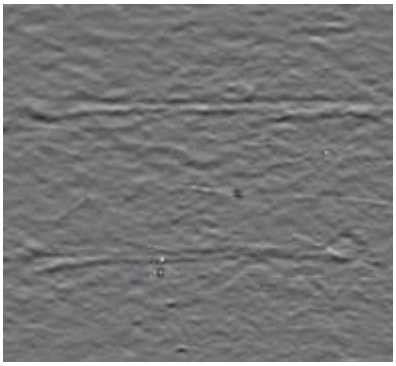

Figure 19: Panel 25 Curvature Map

In addition, ranking of the curvature maps did not result in a panel order that correlated to the jury results from the visual evaluation of the panels nor did it reduce the amount of variation in juror responses. Consequently, it was determined that the jury evaluation of the curvature maps should not be used to determine the form of the algorithm.

The BLRT Metric

The ONDULO technology is fortunately insensitive to the surface characteristics that made it impossible to visually evaluate the raw and white panels. The objective of this project is to extract the curvature data in a way that properly ranks the defect severity of these defects so that the results correlate with visual inspection. While the surface finish of the sample impacts a person's perception of the severity of the defect, the metric will not account for this effect. Instead, users will be expected to recognize the effect of surface finish when applying the metric to production situations.

While the panels manufactured for this work were bonded with continuous beads of adhesive, the defects seen in these samples also included drop and shape defects that must be considered. Because the perceived quality of a surface is a sum of all the data received by our cortico-visual system, we can't avoid being impacted by the occurrence of defects other than stereotypical BLRT even if the operator attempts to concentrate only on BLRT. Moreover, the ability of a person's short-term visual memory to differentiate and rank the different defects is not equivalent for all observers. Consequently, one of the challenges of this project was to consider all the morphological signatures of the defects present on the panels and weigh their severity in a way that correlates with the "average" visual perception.

In deflectometry the objective is to identify an "abnormal" distortion in the reflected light pattern on a surface. "Real" parts, however, are not flat but have some designed shape. Thus the challenge for an automated system is to differentiate the distortion due to the normal, designed shape of the surface from an abnormal distortion that is due to an appearance defect. Human observers who evaluate surface quality instinctively observe only those light distortions that occur over short distances. From this observation, we learn that it is the high frequency component which must be extracted from the curvature field to identify defects as illustrated in Figures 4 and 5.

The first step in evaluating a defect of interest is to determine the wavelength range in which it appears. Once the wavelength range has been selected, the first appropriate mathematical operation to perform is to identify which pixels in an image exceed a particular curvature

amplitude threshold. By thresholding, the pixels that exceed the threshold are then identified as possible defects. The challenge is to identify a threshold that corresponds to the defects that are “visible”.

After pixels which exceed a selected threshold are identified, adjoining pixels are grouped as a single defect. Defects below a certain size, in mm^2, are omitted through a filtering operation. Finally, for panels bonded together using a continuous bead of adhesive, defects below a certain aspect ratio are again omitted using a filtering operation. These size and aspect ratio filters remove the defects that do not appear to be related to BLRT and help to discriminate the severity of the different bonding defects. The magnitude for the filters was chosen based on how well the resulting score correlated with the visual jury results.

The algorithm rates a defect using a score that defines both the signature and the severity of that defect. The score is calculated by the defect’s mean curvature amplitude weighted by its size and its aspect ratio. The score for a panel is then the sum of the scores of all defects on the panel.

One should note that several types of defects can be created in the bonding process. These defects can be classified based on their unique characteristics. The different types of defects encountered have been labelled Bond Line Read Through (BLRT), Bond Drop Read Through (BDRT), and Bond Shape Read Through (BSRT). The characteristics of each are defined as follows:

- BLRT: medium amplitude curvature, medium surface size, high aspect ratio,
- BDRT: high amplitude curvature, low surface size, low aspect ratio,
- BSRT: low amplitude curvature, high surface size, medium aspect ratio.

Defects of different characteristics have differing “apparent” severity. For instance, a small BDRT would be considered to be an “objectionable” defect at a smaller size than a BLRT. Similarly, a defect with characteristics that would be classified as a BLRT will be more “objectionable” to an observer than a similar size BSRT. One solution for accounting for the different apparent severities of the different types of defects is to “weight” each defect score by an arbitrary factor or by a “geometrical” factor, such as curvature amplitude.

Thus, the metric tool has been developed to detect, filter, score and rank all the bonding read-through defects by performing the following operations:

- **Project manager**: Records the measurement configuration (acquisition process, setup, distances between light pattern, measured surface and sensor, etc).
- **Acquisition**: Acquires both horizontal and vertical phase shiftings to detect bonding defects in all directions (horizontal, vertical, diagonal and circular).
- **Derivation**: Combines the acquired phase maps and then derives the curvatures to generate the total curvature map.
- **Perspective correction**: Corrects the perspective view between the camera and the measured surface via an automatic procedure to generate a plan view of the surface to allow the defects on the panel to be more easily located.
- **Masking**: Selects the regions of interest to clean the acquired image of unrelated measurements such as edges and character lines designed as part of the surface (high curvature values).

- **Scaling**: Defines the minimum and maximum values for the map by 1) automatically setting the same minimum and maximum values for all maps, 2) automatically setting the scale based on the map's mean value, or 3) by allowing the user to choose the minimum and maximum limits of the curvature scale for each map.
- **Filtering**: Completes a frequency analysis to identify the wavelength range of the defects.
- **Thresholding**: Analyzes the parameters which define each defect signature (curvature amplitude in m^{-1} lateral size in mm^2, aspect ratio in %, etc).
- **Ranking score**: Weighting of the parameters to establish a score for each defect.
- **Single button functionality**: Saves the analysis so that is can be performed automatically by an inexperienced operator.

Correlation of the BLRT Metric to Visual Assessment

The final weighting factors necessary to achieve the best possible correlation to the jury data have not yet been identified. Nevertheless, the initial algorithm resulted in good correlation between the BLRT scores and the jury data for the primed and painted black panels. This algorithm considered the curvature data in the 5-20mm wavelength range. Pixels with relative curvature amplitude greater than 0.40 deg[†] were included as possible defects. Defects resulting from agglomeration of those pixels were included in the score calculation if the defect as a whole had mean curvature amplitude of 0.40 deg, size greater than $50mm^2$, and aspect ratio greater than 4.75.

The BLRT scores for the primed panels and painted black panels are shown in Figures 20 and 21. The panels rank from the visual evaluation is shown below the panel ID in these figures for reference.

BLRT Score	1.6	6.7	7.6	8.1	8.2	8.6	15.3	17.6	20.9	40.1	62.6	63.0
Panel ID#	59	62	5	17	44	26	32	47	41	11	29	35
Visual Rank	1	2	3	4	5	6	7	8	9	10	11	12

Figure 20: BLRT Scores for the Primed Panels Using the Initial Algorithm

BLRT Score	8.3	9.4	9.7	10.2	11.5	12.7	20.3	34.8	45.0	48.1	76.9	84.5
Panel ID#	39	45	3	18	42	48	21	6	24	30	36	12
Visual Rank	2	1	7	4	6	9	5	3	8	10	12	11

Figure 21: BLRT Scores for the Painted Black Panels Using the Initial Algorithm

The initial algorithm was able to replicate the jury's ranked order in the set of primed panels. Figure 22 shows all twelve panels in this set in ranked order with their BLRT score. This figure shows that the order as determined by the jury "makes sense" relative to the curvature maps captured by the ONDULO technology and that the relative severity as defined by the BLRT score for each panel also "makes sense".

[†] An earlier version of the software was used to create the initial algorithm. At that time, the relative curvature values (in degrees) were used. Since that time the software has been updated to automatically calculate the setup parameters. Consequently, the absolute curvature values (in m^{-1}) are now used.

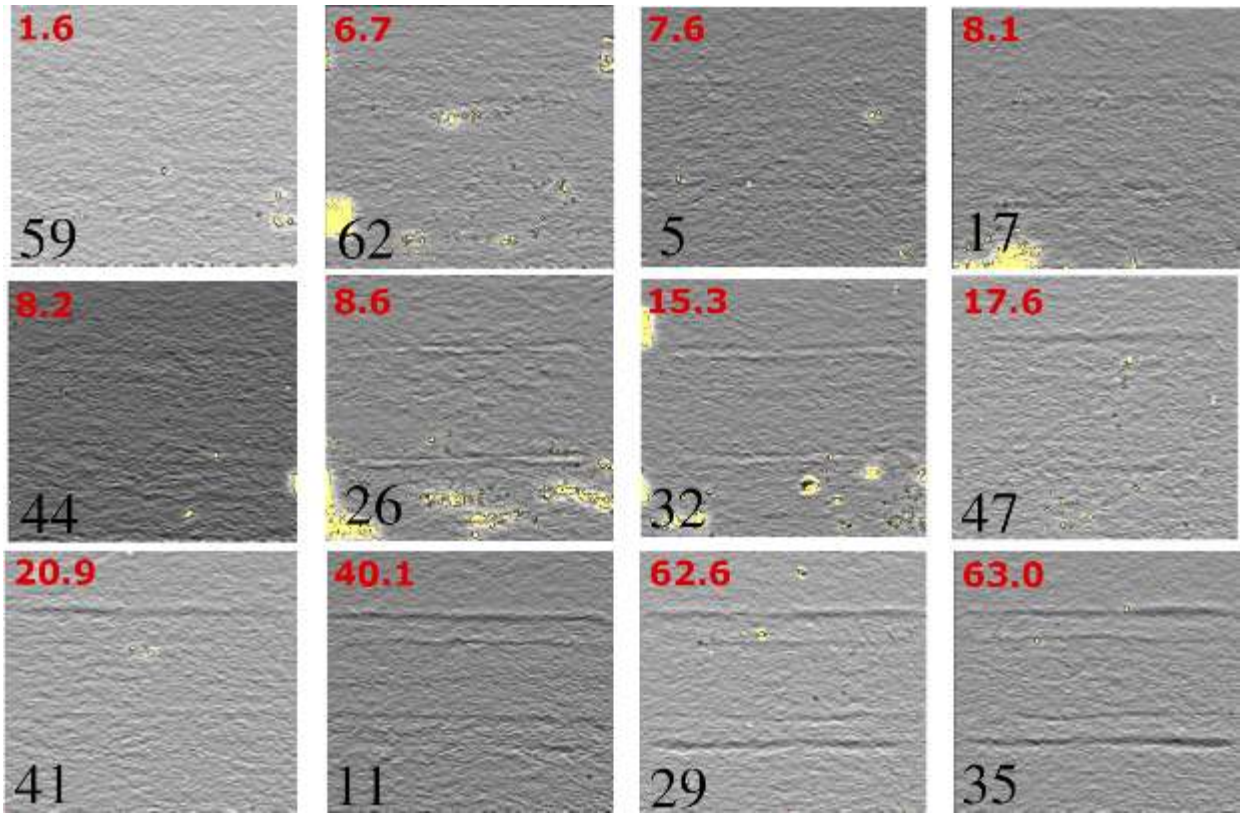

Figure 22: BLRT Images and Scores for the Primed Panels Using the Initial Algorithm

The panel ranking generated by the algorithm scores does differ from the average jury ranking for the set of painted black panels (see Figure 21). This, however, is not surprising given the amount of scatter in the jury data and the issues with the jury evaluation discussed earlier. Figure 23 shows the twelve panels in this set in the order determined by their BLRT score calculated using the initial algorithm. For the most part, the order of the panels in this figure "makes sense" when compared with the directional information available from the jury evaluation. Specifically, panels that were visually ranked as "better" typically had low scores, while panels visually ranked as "worse" typically had high scores. It is the panels in the middle of the distribution that had visual rankings that were statistically indistinguishable that are found to be in a different order. The score and relative ranking of panel #3 and panel #12 in this set, however, indicated that the algorithm needed to consider additional factors.

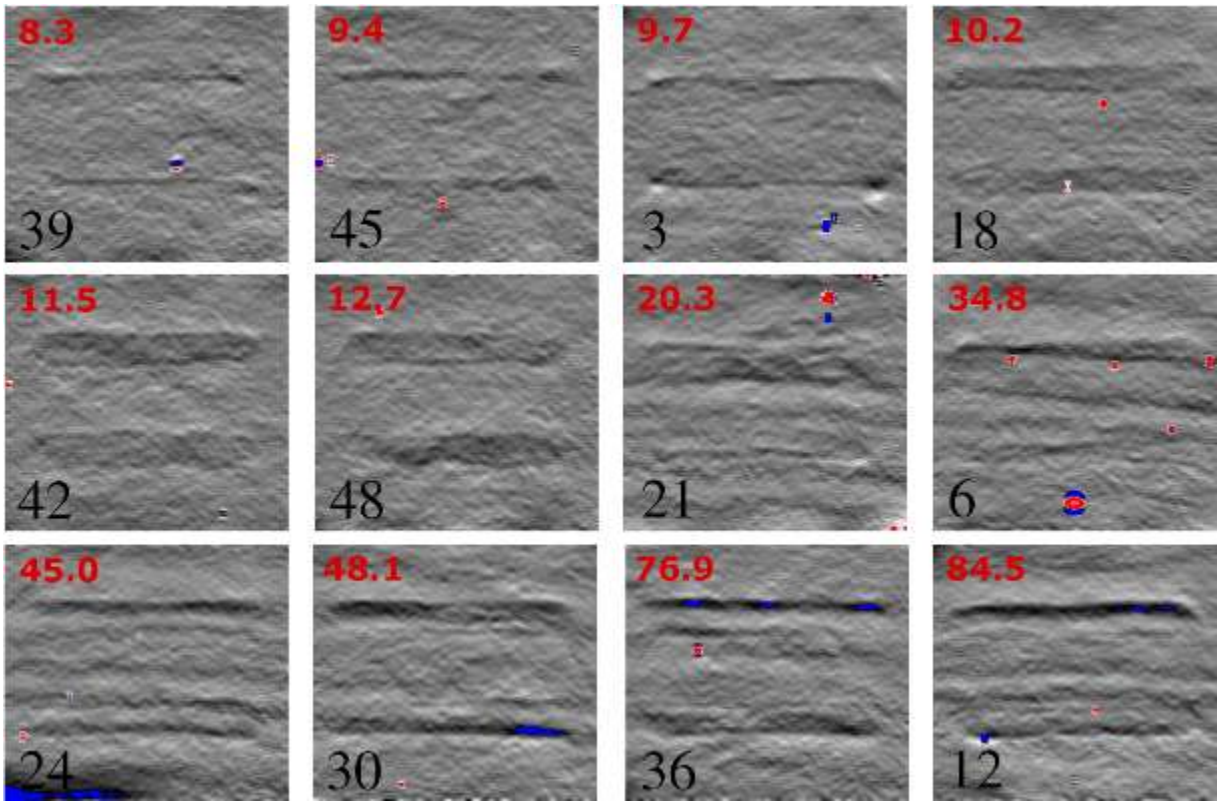

Figure 23: BLRT Images and Scores for the Painted Black Panels Using the Initial Algorithm

In the image of panel #3 in Figure 23, there are small, high amplitude, circular defects that are quite visible on the actual panel. The composition of the initial algorithm was such that these defects are not identified nor included in the panel score. Because these defects are so visible, the algorithm must be modified to both identify and more heavily weigh this type of defect.

In the image of panel #12 in Figure 23, there is a relatively large, "secondary" shape defect directly above a "primary" linear defect at the top of the panel (the light-colored area above the dark line). This "shape" defect contributes substantially to the score for this panel although it did not appear to heavily influence the jurors' assessment of this panel given that panel #36 was usually chosen as the "worst" panel in the set. This defect does exist in the panel and it is possible that observers would consider this defect to be objectionable if it existed independently of the adjacent linear defect. Consequently, the team has decided not to attempt to modify the algorithm to specifically reduce the impact of that defect on this panel's score, but rather will assess the impact of future changes in the algorithm on the scoring of this defect. If changes made to the algorithm to address other issues also reduce the contribution of this defect to the score of panel #12, this would indicate that the overall correlation of the algorithm to the jury assessment has improved.

Although the primary requirement for the measurement tool was that it generates a "score" that correlates to visual assessments, the fact that the technology is insensitive to surface characteristics is valuable in that it allows for measurement of defects that are below the visibility limit. While this will require additional care when establishing requirements for BLRT, it will allow one to properly determine which factor created a BLRT defect rather than simply identifying the processing factor(s) that made the defect visible.

Nonetheless, the fact that the ONDULO system is insensitive to some of the surface characteristics that determine a defect's visibility must be considered when setting BLRT acceptability requirements. For the purposes of this project, however, the requirement for the measurement is only that it correlates with visual assessment of panels made with a single type of surface preparation, including paint color.

Summary

A metric for quantifying the severity of BLRT defects was developed based on the ONDULO technology. A first iteration of the metric generally correlated well with visual assessment of the panels evaluated in this work. This metric was based on the mean curvature amplitude of individual defects weighted by their size and aspect ratio. Since the panels used to develop the first iteration of the metric were all made with continuous beads of adhesive, the initial version of the metric did not properly assess small, high amplitude defects or circular defects. Consequently, further refinement of the algorithm is ongoing. Based on the results shown here for linear defects, though, the team has high confidence that a future iteration of the algorithm will produce a metric that properly quantifies all types of bonding related defects. In addition, since the metric is based on measured physical characteristics of defects, it eliminates the subjectivity inherent in current assessment techniques. The metric, once complete, will provide the objective data necessary to conclusively identify the process and material variables that cause BLRT defects.

Acknowledgements

This material is based upon work supported by the Department of Energy National Energy Technology Laboratory under Award Number DE-FC26-02OR22910.

The authors would like to thank Brad Haskell at Continental Structural Plastics for providing us with the SMC panels and hat sections used in this work and for priming the bonded assemblies. The authors also thank Lord Corporation for providing the adhesive used to manufacture the panels.

References

1. S. R. Durso, S. E. Howe and M. W. Pressley, “Adhesive Bond-line Read-through: Theoretical and Experimental Investigations,” *SAE Technical Paper Series* **1999**, SAE-1999-01-0984.
2. C. C. Lee, “A Finite Element Study of Bond-Line-Read-Out,” *Journal of Reinforced Plastics & Composites* **1995**, *14*, 11, 1226-1249.
3. O. Hahn and J. Jendrny, “Evaluation on simulation models for the estimation of deformation of adhesively bonded steel sheets during curing,” *Welding In The World* **2003**, *47*, 7-8, 31-38.
4. O. Hahn and T. Orth, “Avoiding Bondline Readthrough on Thin Steel Modification and Optimization of Processes, Adhesives and Sample Shape,” *International Body Engineering Conference and Exposition*, Stuttgart, Germany, Sept. 30 – Oct. 2, **1997**, 111-115.